

# Effect of the back surface topography on the efficiency in silicon solar cells

Guo Aijuan(郭爱娟)<sup>1,†</sup>, Ye Famin(叶发敏)<sup>1</sup>, Guo Lihui(郭里辉)<sup>2</sup>, Ji Dong(纪冬)<sup>2</sup>,  
and Feng Shimeng(冯仕猛)<sup>1</sup>

(1 Solar Energy Institute, Department of Physics, Shanghai Jiaotong University, Shanghai 200240, China)

(2 Shanghai Topsolar Green Energy Co., Ltd, Shanghai 200240, China)

**Abstract:** Different processes are used on the back surface of silicon wafers to form cells falling into three groups: textured, planar, and sawed-off pyramid back surface. The characteristic parameters of the cells,  $I_{SC}$ ,  $V_{OC}$ , FF, Pm, and  $E_{ff}$ , are measured. All these parameters of the planar back surface cells are the best. The FF, Pm, and  $E_{ff}$  of sawed-off pyramid back surface cells are superior to textured back surface cells, although  $I_{SC}$  and  $V_{OC}$  are lower. The parasitic resistance is analyzed to explain the higher FF of the sawed-off pyramid back surface cells. The cross-section scanning electron microscopy (SEM) pictures show the uniformity of the aluminum–silicon alloy, which has an important effect on the back surface recombination velocity and the ohmic contact. The measured value of the aluminum back surface field thickness in the SEM picture is in good agreement with the theoretical value deduced from the Al–Si phase diagram. It is shown in an external quantum efficiency (EQE) diagram that the planar back surface has the best response to a wavelength between 440 and 1000 nm and the sawed-off back surface has a better long wavelength response.

**Key words:** planar back surface; aluminum–silicon contact; back surface field

**DOI:** 10.1088/1674-4926/30/7/074003

**PACC:** 8160; 7340C; 8630J

## 1. Introduction

The texturization method, i.e., forming pyramids on the silicon wafer surface, is widely used in current mass-scale production. It can increase the optical path length and reduce reflections, which is necessary to increase the photocurrent and leads to a higher conversion efficiency. In the case of monocrystalline silicon solar cells, a mixture of alkaline solutions, such as sodium hydroxide or potassium hydroxide and isopropyl alcohol, is usually used for texturing<sup>[1,2]</sup>. Depositing an aluminum layer on the back surface of solar cells by screen printed technology is also an effective method to improve the efficiency. A highly Al-doped p<sup>+</sup> region induces a BSF effect, which lowers the effective back-surface recombination velocity<sup>[3]</sup> and improves the collection probability of minority carriers. Al gettering of defects and impurities can increase the minority carrier diffusion length in the bulk<sup>[4]</sup>. Industrial texturing technology forms pyramids not only on the front surface, but also on the back surface of solar cells. Actually, the Al-BSF covers the rough textured surface. It has been shown that rapid thermal processing can reduce the difference between a planar and a textured BSF<sup>[5]</sup>.

In this paper we investigate three groups of silicon wafers made by identical commercial production techniques except for different processes on the back surface. The characteristic parameters of the cells,  $I_{SC}$ ,  $V_{OC}$ , FF, Pm, and  $E_{ff}$ , are measured and compared. The BSF quality is analyzed by taking cross-sectional SEM pictures and the EQE.

## 2. Experiment

We chose 125 × 125 cm<sup>2</sup> p-type CZ Si <100> wafers with 200 μm thickness, 2–3 Ω·cm resistivity, and 1.65 μs minority carrier lifetime. All these wafers were divided into three groups.

Figure 1 shows the flow chart of the experiment carried out by a commercial cell fabrication. For three groups of wafers, different processes were used on the back surface. Group 1: textured back surface, where both sides were textured to form pyramids. Group 2: planar back surface, where only

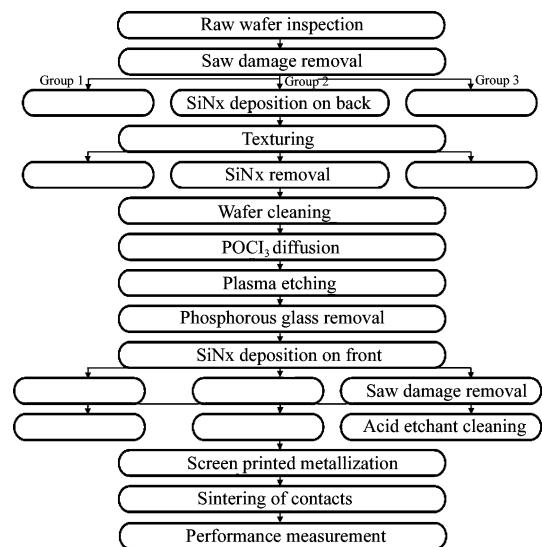


Fig. 1. Flow chart of the experiment.

† Corresponding author. Email: amyy\_088@163.com

Received 19 June 2008, revised manuscript received 30 December 2008

© 2009 Chinese Institute of Electronics

Table 1. Comparison of characteristic parameters.

Parameter	Group 1	Group 2	Group 3
$I_{SC}$ (A)	5.165	5.192	5.155
$V_{OC}$ (mV)	614.6	615.4	614.4
FF	0.737	0.752	0.747
Pm (W)	2.340	2.402	2.367
$E_{ff}$ (%)	16.01	16.43	16.19

Table 2. Ratios of the calculated  $R_{CH}$  to the measured  $R_{SH}$  and  $R_S$ .

Parameter	Group 1	Group 2	Group 3
$R_S$ ( $\Omega$ )	0.01136	0.01074	0.01072
$R_{SH}$ ( $\Omega$ )	7.210	8.096	7.645
$R_{CH}$ ( $\Omega$ )	0.1190	0.1185	0.1192
$R_{CH}/R_S$	10.47	11.04	11.12
$R_{SH}/R_{CH}$	60.67	68.31	64.14

the front surface was textured by using  $\text{SiN}_x$  as a protection mask of the back surface. Group 3: sawed-off pyramids back surface; first, textured on both sides, and then sawed the back surface pyramids a little after  $\text{SiN}_x$  anti-reflection coating was deposited on the front surface. The characteristic parameters and the EQE were measured by a SPI-CELL TESTER and 7-SolarSpec I (DR003), respectively.

### 3. Results and discussion

In this experiment, the saw damage removal step and the texturing step reduced the thickness of the wafers. The thickness of the wafers was measured twice: during the raw wafers inspection and before the diffusion. The average thickness reductions of the three groups were 22.158, 11.758, and 23.177  $\mu\text{m}$ . Obviously, Group 2 is advantageous for producing thinner cells because of the reduced waste.

Table 1 shows the average comparison of the characteristic parameters of the three groups of cells. Each parameter of the cells from Group 2 is the best among all the three groups. This shows that planar back surface cells are superior to textured back surface cells. Although  $I_{SC}$  and  $V_{OC}$  of Group 1 are better than for Group 3, FF, Pm, and  $E_{ff}$  are lower.

The characteristic resistance of a solar cell<sup>[6,7]</sup> is defined as

$$R_{CH} = \frac{V_{OC}}{I_{SC}}. \quad (1)$$

Table 2 shows the measured shunt resistance  $R_{SH}$ , serial resistance  $R_S$ , the calculated  $R_{CH}$ , and the ratios of the calculated  $R_{CH}$  to the measured  $R_{SH}$  and  $R_S$ , respectively. If  $R_S \ll R_{CH}$  or  $R_{SH} \gg R_{CH}$ , the parasitic resistance will have little effect on the FF<sup>[8]</sup>. As we see in Table 2,  $R_{CH}$  is about 10 times greater than  $R_S$  while  $R_{SH}$  is over 60 times greater than  $R_{CH}$ . This means,  $R_S$  has a stronger effect on FF than  $R_{SH}$  does. The normalized voltage  $v_{OC}$ , the approximate expression of FF<sub>0</sub>, and the fill factor FF, considering the effect of  $R_S$ , can

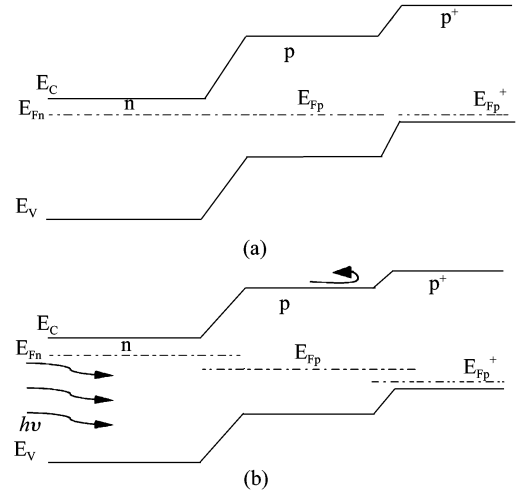


Fig. 2. Energy band schematic diagram of the n/p-p<sup>+</sup> junction (a) at thermal equilibrium and (b) under illumination.

be calculated by<sup>[8]</sup>

$$v_{OC} = \frac{V_{OC}}{nkT/q}, \quad (2)$$

$$FF_0 = \frac{v_{OC} - \ln(v_{OC} + 0.27)}{v_{OC} + 1}, \quad (3)$$

$$FF = FF_0 \left(1 - \frac{R_S}{R_{CH}}\right), \quad (4)$$

where the ideality factor  $n$  is between 1 and 2,  $k$  is Boltzmann's constant,  $T$  is the absolute temperature, and  $q$  is the absolute value of the electron charge. Under standard testing conditions with the air mass (AM) 1.5,  $T = 300$  K,  $k = 1.38 \times 10^{-23}$  J/K,  $q = 1.602 \times 10^{-19}$  C, and  $n = 1$ . The FF values of the three groups are calculated to be 0.751, 0.756, and 0.756, respectively. This explains the effect of  $R_S$  on FF, which makes the FF of Group 3 larger than that of Group 1 while  $V_{OC}$  is lower.

Long wavelength light is absorbed near the back surface. The highly Al doped p<sup>+</sup> region induces a BSF effect, which is a good back reflector of long wavelength light. Figure 2 shows the energy band schematic diagram of the n/p-p<sup>+</sup> junction. The p-p<sup>+</sup> junction forms a potential barrier, which prevents photo-generated minority carriers from flowing into the p<sup>+</sup> region.

Figure 3 shows a cross-section SEM picture of the three groups of wafers. The theoretical value of the Al BSF thickness deduced from the Al-Si phase diagram is calculated using the following formula<sup>[9]</sup>:

$$W_{BSF} = \frac{t_{Al}\rho_{Al}}{\rho_{Si}} \left[ \frac{F(T)}{1-F(T)} - \frac{F(T_0)}{1-F(T_0)} \right], \quad (5)$$

where  $t_{Al}$  is the thickness of the deposited Al,  $\rho_{Al}$  and  $\rho_{Si}$  represent the densities of Al and Si,  $F(T_0)$  and  $F(T)$  are the Si atomic weight percentages in the molten phase, respectively, at the peak alloying and eutectic temperature. In this study, an Al paste is screen-printed with a resulting thickness of  $\sim 30$   $\mu\text{m}$  followed by alloying at 850  $^\circ\text{C}$ . The theoretical  $W_{BSF}$  is calculated to be  $\sim 12$   $\mu\text{m}$  using Eq. (5). In Fig. 3(a), the BSF

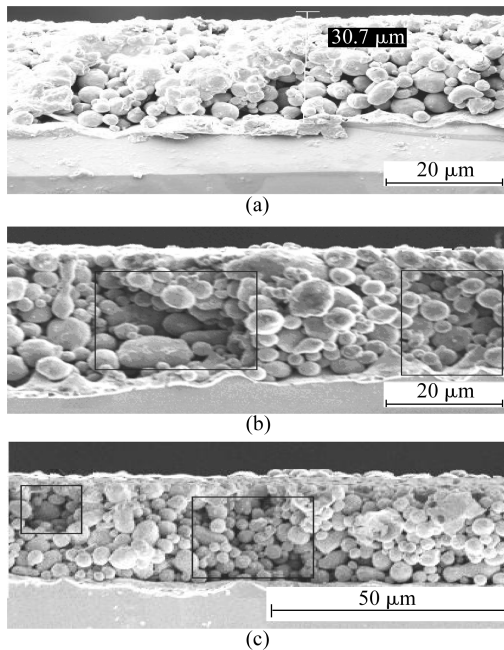


Fig. 3. Cross-section SEM pictures of the three groups of wafers: (a) Group 2, planar back surface; (b) Group 1, textured back surface ; (c) Group 3, sawed-off pyramid back surface.

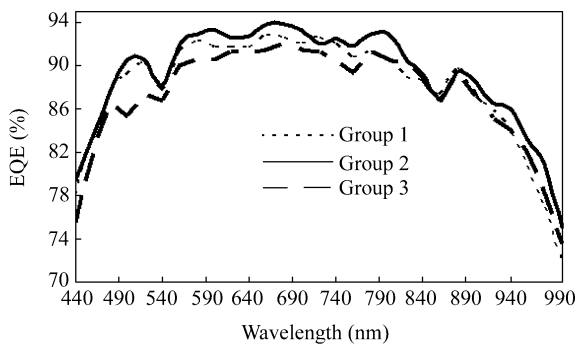


Fig. 4. 400–1000 nm EQE response of the three groups.

thickness is about 13–14  $\mu\text{m}$ , which is in agreement with the theoretical value.

As shown in Figs. 3(b) and 3(c), the uniformity of the Group 1 Al–Si alloy is inferior to that of Group 3. It reveals textured back surface results in larger scale unconnected section (marked by rectangle) than sawed-off pyramids back surface does. Compared with Fig. 3(a), the planar back surface obtains the best uniformity on the Al–Si alloy. Poor uniformity will increase the dangling bonds and surface defect states density, which result in a higher back surface recombination velocity. When the surface state density is very high, the barrier height is decided by the surface quality, almost independent of the metal work function<sup>[10]</sup>. Therefore, the poor uniformity also degrades the BSF effect and the ohmic contact. The cross-section SEM pictures are in good agreement with the measured characteristic parameters given in Table 1.

Figure 4 shows the EQE response of the three groups from 440 to 1000 nm. Clearly, Group1 has the best response to all the wavelengths. It reveals that the planar back surface not only improves the absorption of longer wavelengths near the

back surface, but also improves absorption in the bulk. From 440 to 790 nm, the EQE response of Group 3 is inferior to Group 1, which is attributed to its poor  $I_{\text{SC}}$  and  $V_{\text{OC}}$ . However, Group 3 has better an EQE response to wavelengths longer than 940 nm, which is due to the sawed-off pyramids back surface.

#### 4. Conclusion

In this study, we have shown that the topography of the back surface plays an important role for improving the performance of solar cells. Planar back surface cells improve the cell performance as seen by measuring the parameters  $I_{\text{SC}}$ ,  $V_{\text{OC}}$ , FF,  $P_m$ , and  $E_{\text{ff}}$ . They have good BSF, better uniformity of the Al–Si alloy, and better EQE response. Compared with a textured back surface, the sawed-off pyramid back surface improves the uniformity of the Al–Si alloy and has good long wavelength EQE. Moreover, the sawed-off pyramid back surface can obtain a higher FF,  $P_m$ , and  $E_{\text{ff}}$  due to its better  $R_s$ .

#### References

- [1] King D L, Buck M E. Experimental optimization of an anisotropic etching process for random texturization of silicon solar cells. Proceedings of the 22nd IEEE Photovoltaic Specialists Conference, 1991: 303
- [2] Vazsonyi E, De Clercq K, Rinhaus R, et al. Improved anisotropic etching process for industrial texturing of silicon solar cells. Solar Energy Materials and Solar Cells, 1999, 57(2): 179
- [3] Lolgen P, Leguijt C, Eikelboom J A, et al. Aluminum back-surface field doping profiles with surface recombination velocities below 200 cm/s. Proceedings of the 23rd IEEE Photovoltaic Specialists Conference, 1993: 236
- [4] Subhash M J, Ulrich M G, Teh Y T. Improvement of minority carrier diffusion length in Si by Al gettering. J Appl Phys, 1995, 77(8): 3858
- [5] Meemongkolkiat V, Hilali M, Rohatgi A. Investigation of RTP and belt fired screen printed Al-BSF on textured and planar back surfaces of silicon solar cells. Proceedings of the 3rd World Conference on Photovoltaic Energy Conversion, 2003: 1467
- [6] Fossum J G, Nasby R D, Pao S C. Physics underlying the performance of back-surface-field solar cells. IEEE Trans Electron Devices, 1980, 27(4): 785
- [7] Green M A. General solar cell curve factors including the effects of ideality factor, temperature and series resistance. Solid State Electron, 1977, 20: 265
- [8] Green M A. Solar cells: operating principles, technology, and system applications. United States: Prentice-Hall, Inc., Englewood Cliffs, NJ, 1982
- [9] Alamo J D, Eguren J, Luque A. Operating limits of Al-alloyed high-low junctions for BSF solar cells. Solid-State Electron, 1981, 24: 415
- [10] Liu Enke, Zhu Bingsheng, Luo Jinsheng. Semiconductor physics. Xi'an Jiaotong University, 1998